Filtration and Extraction of Quantum States from Classical Inputs

Chang-Ling Zou[1,2,3], Liang Jiang[2],* Xu-Bo Zou[1,3],† and Guang-Can Guo[1,3]
[1] *Key Lab of Quantum Information, University of Science and Technology of China, Hefei 230026*
[2] *Department of Applied Physics, Yale University, New Haven, CT 06511, USA and*
[3] *Synergetic Innovation Center of Quantum Information & Quantum Physics, University of Science and Technology of China, Hefei, Anhui 230026, China*

(Dated: August 18, 2015)

We propose using nonlinear Mach-Zehnder interferometer (NMZI) to efficiently prepare photonic quantum states from a classical input. We first analytically investigate the simple NMZI that can filtrate single photon state from weak coherent state by preferrentially blocking two-photon component. As a generalization, we show that the cascaded NMZI can deterministically extract arbitrary quantum state from a strong coherent state. Finally, we numerically demonstrate that the cascaded NMZI can be very efficient in both the input power and the level of cascade. The protocol of quantum state preparation with NMZI can be extended to various systems of bosonic modes.

Introduction.- Integrated photonics can achieve unprecedented interferometric stability [1, 2] and build large scale interferometers [3, 4]. However, reliable quantum state preparation for integrated photonics remains an important challenge, because interferometers and coherent input states are insufficient for quantum states preparation. We may use either post-selection or nonlinear interaction to overcome this challenge. The approach of post-selection only requires linear optical elements and photon detectors, but the preparation of quantum state is probabilistic and conditioned on the outcome of the projective measurement [5–7]. The approach of nonlinear interaction assisted by an ancillary two-level system (TLS) can deterministically prepare arbitrary quantum state of the photonic mode [8–10], but it requires strong coupling between the optical mode with the single TLS, which is experimentally challenging for integrated photonics. Alternatively, we may consider using the nonlinear optical waveguide combined with ultra-stable interferometers to achieve reliable quantum state preparation, without requiring TLS [8–10], post-selection [11–13], nor feedback/feedforward control [14].

In this Letter, we propose to use interferometry combined with Kerr nonlinearity to filtrate single photons or extract any desired quantum states from coherent state input, as illustrated in Fig. 1(a). We first present the idea of quantum state filtration (QSF) of single photons, which keeps the desired single photon component by *blocking* the undesired component to a different port. We then generalize the idea to quantum state extraction (QSE), which not only keeps the desired component, but also extracts the desired component from the undesired component before blocking/redirecting the residual photons.

Single photon filtration.- We first consider the simple task of QSE of single photons. As shown in Fig. 1(b), we use a nonlinear Mach–Zehnder interferometer (NMZI), with a Kerr nonlinear medium in one of the arms. Since Kerr nonlinearity can induce photon number dependent phase shift, we can design the NMZI to induce destructive interference at the output port when there are two photons. More specifically, with a vacuum input at Path A (upper path) and a coherent state input at Path B (lower path), the input state to the filtration is

$$|\psi\rangle_{in} = |vac\rangle_A \otimes |\alpha\rangle_B , \tag{1}$$

where $|\alpha\rangle = e^{-|\alpha|^2/2}\sum_{n=0}^{\infty}\frac{\alpha^n}{n!}(b^\dagger)^n|vac\rangle$, and $a(a^\dagger)$ and

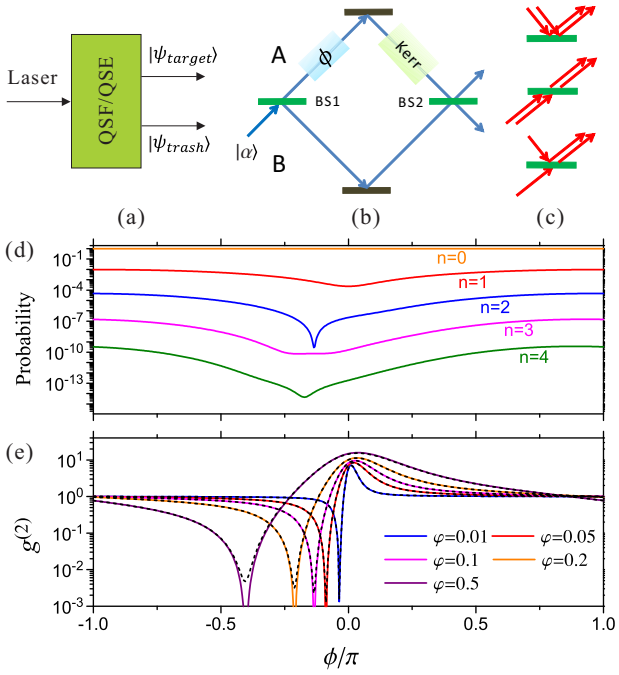

Figure 1: (color online) (a) Schematic illustration the arbitrary quantum state filtration and extraction from coherent state input. (b) The configuration for QSF of single photon from coherent state input $|\alpha\rangle$, using the simple NMZI (consisting of Mach–Zehnder interferometer, and Kerr medium and phase shifter). (c) Three processes for two photon output of Path A for weak coherent input. (d) The probabilities of n photons output of Path A against the phase difference between two arms ϕ, with $\varphi = 0.1$ and $\alpha = 0.1$. (e) The second-order correlation function ($g^{(2)}$) of light output of Path A against ϕ for various φ with $\alpha = 0.1$.

$b(b^\dagger)$ are annihilation (creation) operators for Paths A and B, respectively. Each beam splitter (BS) induces a unitary evolution,

$$U_{BS}(\theta_{1,2}) = e^{i\theta_{1,2}(a^\dagger b + a b^\dagger)}, \tag{2}$$

with θ_1 and θ_2 for BS1 and BS2, respectively. The evolution in the nonlinear Kerr medium in Path A is

$$U_K(\phi,\varphi) = e^{i\phi a^\dagger a + i\varphi a^\dagger a^\dagger a a}, \tag{3}$$

where φ is the Kerr coefficient and ϕ is linear phase shift (relative to Path B). The final output state of the single photon filtration is

$$\begin{aligned} |\psi\rangle_{out} =& U_{BS}(\theta_2)U_K(\phi,\varphi)U_{BS}(\theta_1)\,|\psi\rangle_{in} \\ =& \sum_{p=0}^{\infty}\sum_{q=0}^{\infty}\mu_{p,q}(a^\dagger)^p(b^\dagger)^q\,|vac\rangle\,, \end{aligned} \tag{4}$$

with $\mu_{p,q} = \sum_{l=0}^{p}\sum_{n=l}^{l+q}\lambda_{n,p+q-n}\binom{n}{l}\binom{p+q-n}{p-l} \times (-1)^{n-l}(\sin\theta_2)^{p+n-2l}(\cos\theta_2)^{q-n+2l}$. The probability of p photons at the output of Path A is

$$P_p = \langle p|\,\mathrm{Tr}_B\{|\psi_2\rangle\langle\psi_2|\}\,|p\rangle = \sum_{q=0}^{\infty} p!q!\,|\mu_{p,q}|^2\,.$$

The second-order correlation function [15] is

$$g^{(2)} = \frac{\langle a^\dagger a^\dagger a a\rangle}{\langle a^\dagger a\rangle^2} = \frac{\sum_{p=2}^{\infty}p(p-1)\times P_p}{(\sum_{p=1}^{\infty}p\times P_p)^2}, \tag{5}$$

which characterizes the generated single photon state.

For a weak coherent input $|\alpha|^2 \ll 1$, we have $P_2 \ll P_1$ and can safely neglect the probability of multiple photons ($P_{n\geq 3}$). By considering the leading contribution, we have

$$g^{(2)} \approx \frac{2P_2}{{P_1}^2} \approx \left|\frac{2\mu_{2,0}}{\mu_{1,0}^2}\right|^2 = \left|1-\frac{1-e^{i2\varphi}}{(1-\eta e^{-i\phi})^2}\right|^2, \tag{6}$$

where $\mu_{1,0} = \alpha\cos\theta_1\cos\theta_2(e^{i\phi}-\eta)$ and $\mu_{2,0} = \frac{1}{2}(\alpha\cos\theta_1\cos\theta_2)^2[-2\eta e^{i\phi}+e^{i2(\phi+\varphi)}+\eta^2]$ for the simple NMZI with $\eta = \tan\theta_1\tan\theta_2$. The three terms in $\mu_{2,0}$ correspond to three different processes with two photons at the output of Path A, as shown in Fig. 1(c). The interference of these three processes can be controlled by the linear phase shift (ϕ) and nonlinear coefficient (φ). The optimal condition for $\mu_{2,0}=0$ is

$$\eta e^{-i\phi} = 1 \pm \sqrt{1-e^{i2\varphi}}, \tag{7}$$

which can always be fulfilled as long as $\varphi \neq 0$, so that the leading contribution to $g^{(2)}$ can be eliminated.

Fig. 1(d) shows the probability of n photons at the output of Path A (P_n) depending on the linear phase shift ϕ, with parameters $\varphi = 0.1$, $\eta = |1-\sqrt{1-e^{i2\varphi}}|$ and $\alpha = 0.1$. We find that the P_2 is greatly suppressed for $\phi \approx 0.13\pi$, while the dominant single photon emission $P_1 \gg P_{2,3,4}$ is not significantly affected. In Fig. 1(e), the relation between $g^{(2)}$ and ϕ are plotted for different values of nonlinear coefficient φ, with $\alpha = 0.1$ and η given by optimal condition from Eq. (7). We find good agreement between the approximated analytical solution from Eqs. (6)&(7) (solid lines) and the exact numerical solution from Eq. (5) (dashed lines). With increasing nonlinear coefficient φ, the deviation from $g^{(2)}=1$ becomes more significant, due to the Fano interference of the three processes (Fig. 1(c)) contributing to $\mu_{2,0}$. These Fano-like curves show sub-Poisson statistic with $g^{(2)} \approx 0$ for ϕ close to the optimal condition (Eq. (7)), where the two photon output can be totally forbidden due to destructive interference. Meanwhile, we can also find the constructive interference of the two-photon output, which gives rise to super-Poisson statistic ($g^{(2)}(0) \gg 1$) output. Comparing the curves with different nonlinear effect coefficients, the single photon filtration is more sensitive to phase ϕ for smaller φ, indicating the crucial role of nonlinearity.

For QSF of single photon, the fidelity is $F = P_1 = (\cos\theta_1\cos\theta_2)^2|\alpha^2|\,|1-e^{i2\varphi}|$. The optimal condition requires $\eta = \tan\theta_1\tan\theta_2 \approx 1$, we have $|\cos\theta_1\cos\theta_2| < \frac{1}{2}$ and $P_1 < \varphi|\alpha^2|/2$, which implies that the fidelity depends on both the the Kerr nonlinearity coefficient and the intensity of the coherent state input. QSF with simple NMZI cannot suppress the components with $n>2$ photons (see Fig. 1(d) and also Ref. [37]), and it only works for weak coherent state $|\alpha^2| \ll 1$, which significantly limits the fidelity. Moreover, the fidelity of QSF is fundamentally limited by the overlap between the input state and the target state, $P_{succ} < |\langle\psi_{out}|\psi_{in}\rangle|^2$, because it blocks all undesired components. To go beyond this limit, we need to generalize QSF to QSE, which not only keeps the desired component, but also extracts the desired component from the undesired ones.

Cascaded filtration.- To implement QSE, we consider the cascaded NMZI, with a series of NMZIs connected sequentially. As shown in Fig. 2(a), the basic element consists of a BS (θ) followed by a linear phase shifter (ϕ) and a Kerr medium (φ) in the upper path. The basic element can be represented by a standard two-port unitary [Fig. 2(b)]

$$U(\phi,\varphi,\theta) = U_{\mathrm{K}}(\phi,\varphi)U_{BS}. \tag{8}$$

The cascaded MNZI with N elements can be characterized by

$$U_N = \Pi_{l=1}^{N}U(\phi_l,\varphi_l,\theta_l). \tag{9}$$

For example, the simple NMZI (Fig 1(b)) consists of $N=2$ basic elements, with $\phi_2=\varphi_2=0$.

The cascaded NMZI can not only keep the desired single-photon component, but also extract the (desired) single-photon state from (undesired) multi-photon states, as long as there are enough photons in the undesired component. We numerically optimize the fidelity by tuning

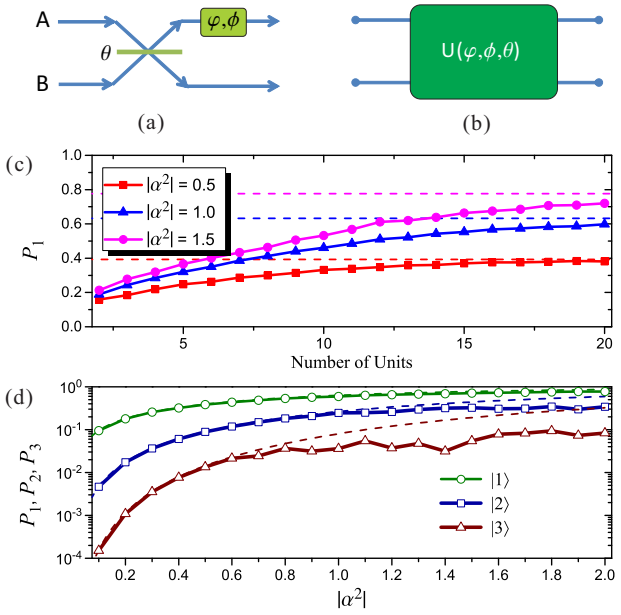

Figure 2: (color online) Cascaded NMZI. (a) The basic element consists of a BS (θ) followed by a linear phase shifter (ϕ) and a Kerr medium (φ) in the upper path. (b) Schematic representation of the element for cascaded NMZI. (c) Fidelity of the single photon extraction increases with the number of cascade elements, N. The parameters are optimized numerically under the constrain $P_{n\geq 2} < 0.01$ with $\varphi = 0.1$. (d) Fidelity of Fock state extraction ($n = 1, 2, 3$) increase with $|\alpha|^2$ for cascaded NMZI with $N = 40$. The results are obtained by optimize the parameters of each unit under the constrain that $1 - P_0 - P_n \leq 0.01$.

the parameters of the N elements. As illustrated in Fig. 2(c), the optimized fidelity of single photon extraction $F = P_1$ increases with N monotonically, with asymptotic value $F \to 1 - |\langle 0|\alpha\rangle|^2$ (dashed lines), because our passive device cannot extract single photon from the vacuum component. Furthermore, the cascaded NMZI can extract Fock state $|n\rangle$ with $n = 1, 2, 3, \cdots$. The asymptotic fidelity of n-photon extraction is $F \to 1 - \sum_{m=0}^{n-1} |\langle m|\alpha\rangle|^2$, which can be achieved for $|\alpha|^2 \leq 1.5/n$ with cascaded NMZI of $N = 40$ elements, as shown in Fig. 2(d).

Arbitrary state Extraction.-Remarkably, the cascaded NMZI can extract *arbitrary* superposition of Fock states with a large coherent state input ($|\alpha| \gg 1$) with almost perfect fidelity. For $\theta_l \ll 1$ with $l = 1, \cdots, N$, almost all input photons will be guided in Path B, which effectively remains as a coherent state (with small deviation of $O(\theta)$) for all intermediate stages. The effect of each beam splitter to the upper path can be regarded as an effective displacement operation to Path A, as $D(\epsilon_l) = e^{\epsilon_l a^\dagger - \epsilon_l^* a}$ with $\epsilon_l = \alpha\theta_l$ and a small deviation of $O\left(\epsilon_l^2/\alpha^2\right)$ [16]. In addition, the linear phase shift and Kerr nonlinearity can achieve the unitary evolution $U_K(\phi_l, \varphi) = e^{i\phi_l a^\dagger a + i\varphi a^\dagger a^\dagger a a}$. Hence, the cascaded NMZI of N elements can induce the unitary evolution

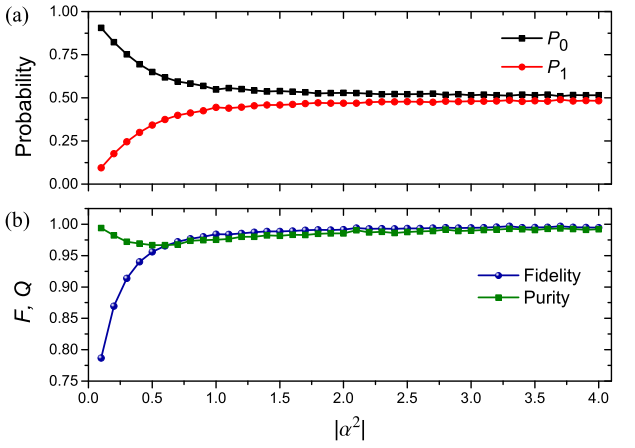

Figure 3: QSE for $|\psi_{target}\rangle = (|0\rangle + |1\rangle)/\sqrt{2}$. (a) The probability of $|0\rangle$ and $|1\rangle$, (b) the Fidelity (F) and Purity (Q) of the output. The results are obtained by optimize the parameters of a chain of $N = 20$ units under the constrain that $1 - P_0 - P_1 \leq 0.01$.

$U_K(\phi_N, \varphi) U(\epsilon_N) \cdots U_K(\phi_2, \varphi) U(\epsilon_2) U_K(\phi_1, \varphi) U(\epsilon_1)$, which in principle can accomplish any desired unitary transformation for sufficiently large N and carefully chosen $\{\phi_l, \epsilon_l\}_{l=1,\cdots,N}$ [17–19]. Despite the large overhead in N, this provides a generic approach using cascaded NMZI to extract arbitrary superposition of Fock states from a large coherent state with almost perfect fidelity.

In practice, it is favorable to design the cascaded NMZI with a small number of elements. To illustrate the feasibility, we consider the target state $|\psi_{target}\rangle = (|0\rangle + |1\rangle)/\sqrt{2}$ using $N = 20$ cascaded elements optimize the fidelity by tuning parameters of $\{\varphi_l, \phi_l, \theta_l\}_{l=1,\cdots,N}$. As illustrated in Fig. 3, we can improve the fidelity F and purity $Q = \mathrm{Tr}(\rho_A^2)$ of the extracted state by increasing $|\alpha|^2$. Both F and Q are greater than 97.5% when $|\alpha|^2 \geq 1.5$. It's intriguing that a high fidelity QSE of superposition of Fock states can be achieved using a reasonable size coherent state and a finite-stage cascaded NMZI.

Discussion.- The photonic integrated circuits (PICs) provides a promising platform for realizing cascaded NMZI, where arrays of beam splitters and phase shifters can be integrated on a chip [3, 4]. QSE can provide arbitrary input photon states for quantum information processing [1, 7]. For experiment realization, the most challenging part is the Kerr nonlinear at single photon level ($\varphi = 0.1$ in this paper). Compared with schemes using single TLS at near-resonance condition, the Kerr nonlinearity can be realized by collective effect of ensembles and is more feasible for experiments. Recently, the interface between atomic ensemble and photonic waveguide for single photon nonlinearity, such as nanofiber [20, 21], hollow-core photonic crystal fiber [22, 23] and integrated waveguide [24], have been deonstrated [25–27]. Novel mechanisms including giant Kerr effect [28]

and strong interaction between Rydberg atoms [29] have also been proposed and demonstrated. As the integrated photonic chips starting the new era of fJ-level (1000 photons) nonlinear effect [30, 31], new materials, such as graphene [32] and topological insulator [33], might enable next generation of PIC with nonlinearity at aJ-level (10 photons). Therefore, the QSE is promising approach for future quantum state generation in PIC.

The idea of QSE can be extended from optical frequency to microwave and terahertz frequencies. In particular, the superconducting quantum circuits is readily to realize the QSE [34, 35]. The mechanism of the QSE is very general, can also be generalized to other Bosonic excitations, such as surface plasmon, exciton-polariton, magnon and phonon. For example, quantum single phonon sources are possible by nonlinear mechanical oscillators [36].

Conclusion.- We have demonstrated that the simple NMZI can filtrate single photon state from a weak coherent state. Using cascaded NMZI, we can reliably extract arbitrary quantum state from a strong coherent state. Since our scheme only requires Kerr nonlinearity, linear phase shifter and beam splitter, it can be implemented in superconducting circuits, coupled optomechanical systems, as well as photonic integrated circuits.

C.L.Z. thanks Hailin Wang and Hong-Wei Li for fruitful discussion. This work is supported by the "Strategic Priority Research Program(B)" of the Chinese Academy of Sciences (Grant No. XDB01030200), National Basic Research Program of China (Grant Nos. 2011CB921200 and 2011CBA00200). LJ acknowledges support from the DARPA Quiness program, the ARO, the AFSOR MURI, the Alfred P Sloan Foundation, and the Packard Foundation.

* Electronic address: liang.jiang@yale.edu
† Electronic address: xbz@ustc.edu.cn

[1] A. Politi, M. J. Cryan, J. G. Rarity, S. Yu, and J. L. O'Brien, "Silica-on-silicon waveguide quantum circuits," Science **320**, 646–649 (2008).
[2] J. L. O'Brien, A. Furusawa, and J. Vučković, "Photonic quantum technologies," Nat. Photonics **3**, 687–695 (2009).
[3] J. Carolan, C. Harrold, C. Sparrow, E. Martin-Lopez, N. J. Russell, J. W. Silverstone, P. J. Shadbolt, N. Matsuda, M. Oguma, M. Itoh, G. D. Marshall, M. G. Thompson, J. C. F. Matthews, T. Hashimoto, J. L. O'Brien, and A. Laing, "Universal linear optics," Science **349**, 711–716 (2015).
[4] N. C. Harris, G. R. Steinbrecher, J. Mower, Y. Lahini, M. Prabhu, T. Baehr-Jones, M. Hochberg, S. Lloyd, and D. Englund, "Bosonic transport simulations in a large-scale programmable nanophotonic processor," arXiv:1507.03406 (2015).
[5] P. Kok, K. Nemoto, T. C. Ralph, J. P. Dowling, and G. J. Milburn, "Linear optical quantum computing with photonic qubits," Rev. Mod. Phys. **79**, 135–174 (2007).
[6] H. M. Chrzanowski, N. Walk, S. M. Assad, J. Janousek, S. Hosseini, T. C. Ralph, T. Symul, and P. K. Lam, "Measurement-based noiseless linear amplification for quantum communication," Nat. Photonics **8**, 333–338 (2014).
[7] E. Knill, R. Laflamme, and G. J. Milburn, "A scheme for efficient quantum computation with linear optics," nature **409**, 46–52 (2001).
[8] C. Law and J. Eberly, "Arbitrary Control of a Quantum Electromagnetic Field," Phys. Rev. Lett. **76**, 1055–1058 (1996).
[9] A. Ben-Kish, B. DeMarco, V. Meyer, M. Rowe, J. Britton, W. M. Itano, B. M. Jelenković, C. Langer, D. Leibfried, T. Rosenband, and D. J. Wineland, "Experimental demonstration of a technique to generate arbitrary quantum superposition states of a harmonically bound spin-1/2 particle," Phys. Rev. Lett. **90**, 037 902 (2003).
[10] M. Hofheinz, H. Wang, M. Ansmann, R. C. Bialczak, E. Lucero, M. Neeley, A. D. O'Connell, D. Sank, J. Wenner, J. M. Martinis, and A. N. Cleland, "Synthesizing arbitrary quantum states in a superconducting resonator," Nature **459**, 546–549 (2009).
[11] X. Zou, K. Pahlke, and W. Mathis, "Linear optical implementation of a single-mode quantum filter and generation of multiphoton polarization entangled states," Phys. Rev. A **66**, 064 302 (2002).
[12] H. F. Hofmann and S. Takeuchi, "Quantum filter for nonlocal polarization properties of photonic qubits," Phys. Rev. Lett. **88**, 147 901 (2002).
[13] K. Sanaka, K. Resch, and A. Zeilinger, "Filtering Out Photonic Fock States," Phys. Rev. Lett. **96**, 083 601 (2006).
[14] C. Sayrin, I. Dotsenko, X. Zhou, B. Peaudecerf, T. Rybarczyk, S. Gleyzes, P. Rouchon, M. Mirrahimi, H. Amini, M. Brune, J.-M. Raimond, and S. Haroche, "Real-time quantum feedback prepares and stabilizes photon number states," Nature **477**, 73–77 (2011).
[15] G. S. Agarwal, *Quantum Optics* (Cambridge University Press, 2012).
[16] M. G. Paris, "Displacement operator by beam splitter," Phys. Lett. A **217**, 78–80 (1996).
[17] D. Deutsch, A. Barenco, and A. Ekert, "Universality in Quantum Computation," Proc. R. Soc. A **449**, 669–677 (1995).
[18] S. Lloyd, "Almost any quantum logic gate is universal," Phys. Rev. Lett. **75**, 346–349 (1995).
[19] S. L. Braunstein, "Quantum information with continuous variables," Rev. Mod. Phys. **77**, 513–577 (2005).
[20] S. M. Hendrickson, M. M. Lai, T. B. Pittman, and J. D. Franson, "Observation of Two-Photon Absorption at Low Power Levels Using Tapered Optical Fibers in Rubidium Vapor," Phys. Rev. Lett. **105**, 173 602 (2010).
[21] E. Vetsch, D. Reitz, G. Sagué, R. Schmidt, S. T. Dawkins, and A. Rauschenbeutel, "Optical Interface Created by Laser-Cooled Atoms Trapped in the Evanescent Field Surrounding an Optical Nanofiber," Phys. Rev. Lett. **104**, 203 603 (2010).
[22] M. Bajcsy, S. Hofferberth, V. Balic, and T. Peyronel, "Efficient all-optical switching using slow light within a hollow fiber," Phys. Rev. Lett. **102**, 203 902 (2009).
[23] V. Venkataraman, K. Saha, P. Londero, and A. L. Gaeta, "Few-Photon All-Optical Modulation in a Pho-

tonic Band-Gap Fiber," Phys. Rev. Lett. **107**, 193 902 (2011).
[24] L. Stern, B. Desiatov, I. Goykhman, and U. Levy, "Nanoscale light-matter interactions in atomic cladding waveguides." Nat. Commun. **4**, 1548 (2013).
[25] D. E. Chang, V. Vuletic, and M. D. Lukin, "Quantum nonlinear optics – photon by photon," Nat. Photonics **8**, 685–694 (2014).
[26] T. G. Tiecke, J. D. Thompson, N. P. de Leon, L. R. Liu, V. Vuletić, and M. D. Lukin, "Nanophotonic quantum phase switch with a single atom," Nature **508**, 241–244 (2014).
[27] A. Goban, C.-L. Hung, S.-P. Yu, J. D. Hood, J. A. Muniz, J. H. Lee, M. J. Martin, A. C. McClung, K. S. Choi, D. E. Chang, O. Painter, and H. J. Kimble, "Atom-light interactions in photonic crystals," Nat. Commun. **5**, 3808 (2014).
[28] H. Schmidt and A. Imamoglu, "Giant Kerr nonlinearities obtained by electromagnetically induced transparency," Opt. Lett. **21**, 1936–1938 (1996).
[29] T. Peyronel, O. Firstenberg, Q.-Y. Liang, S. Hofferberth, A. V. Gorshkov, T. Pohl, M. D. Lukin, and V. Vuletic, "Quantum nonlinear optics with single photons enabled by strongly interacting atoms," Nature **488**, 57–60 (2012).
[30] Y.-D. Kwon, M. A. Armen, and H. Mabuchi, "Femtojoule-Scale All-Optical Latching and Modulation via Cavity Nonlinear Optics," Phys. Rev. Lett. **111**, 203 002 (2013).
[31] M. Notomi, K. Nozaki, A. Shinya, S. Matsuo, and E. Kuramochi, "Toward fJ/bit optical communication in a chip," Opt. Commun. **314**, 3–17 (2014).
[32] M. Gullans, D. Chang, F. Koppens, F. de Abajo, and M. Lukin, "Single-Photon Nonlinear Optics with Graphene Plasmons," Phys. Rev. Lett. **111**, 247 401 (2013).
[33] J. Wang, H. Mabuchi, and X.-L. Qi, "Calculation of divergent photon absorption in ultrathin films of a topological insulator," Phys. Rev. B **88**, 195 127 (2013).
[34] G. Kirchmair, B. Vlastakis, Z. Leghtas, S. E. Nigg, H. Paik, E. Ginossar, M. Mirrahimi, L. Frunzio, S. M. Girvin, and R. J. Schoelkopf, "Observation of quantum state collapse and revival due to the single-photon Kerr effect," Nature **495**, 205–209 (2013).
[35] M. H. Devoret and R. J. Schoelkopf, "Superconducting circuits for quantum information: an outlook," Science **339**, 1169–1174 (2013).
[36] L. Villanueva, R. Karabalin, M. Matheny, D. Chi, J. Sader, and M. Roukes, "Nonlinearity in nanomechanical cantilevers," Phys. Rev. B **87**, 024 304 (2013).
[37] See the Supplemental Material for additional details about the limitation of two-unit NMZI QSF, performance of QSF/QSE for various Kerr nonlinearities and imperfection.

Supplemental Material for

"*Filtration and Extraction of Quantum States from Classical Inputs*"

Chang-Ling Zou[1,2,3], Liang Jiang[2], Xu-Bo Zou[1,3], and Guang-Can Guo[1,3]

[1] *Key Lab of Quantum Information, University of Science and Technology of China, Hefei 230026*

[2] *Department of Applied Physics, Yale University, New Haven, CT 06511, USA*

[3] *Synergetic Innovation Center of Quantum Information & Quantum Physics, University of Science and Technology of China, Hefei, Anhui 230026, China*

Contents

I. LIMITATION OF TWO-UNIT QUANTUM STATE FILTRATION

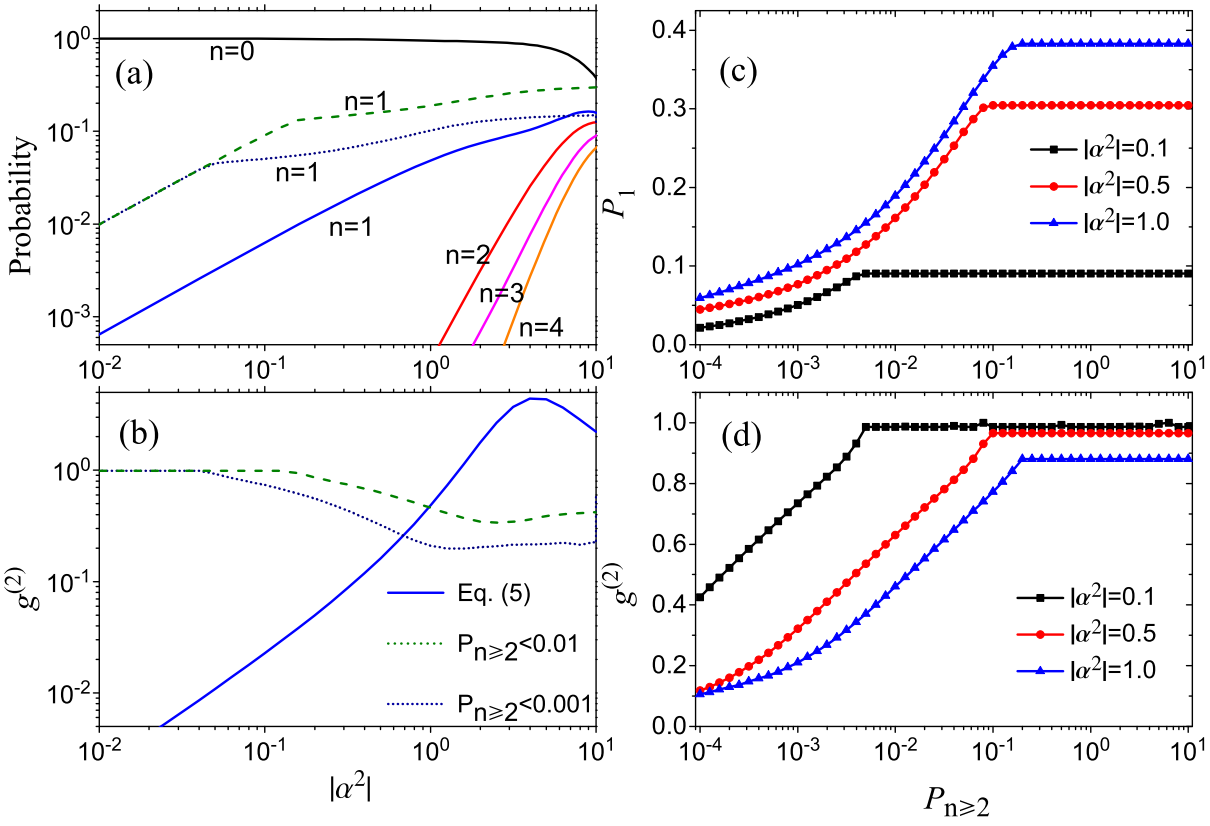

Figure S1: The probability of n-photon (a) and the photon statistic $g^{(2)}$ (b) at output for increasing input coherent laser intensity $|\alpha^2|$. The solid lines are results for optimal conditions from Eq. (7), the dashed lines are numerically optimized results for constrains that $P_{n\geq 2} < 0.01$ and $P_{n\geq 2} < 0.001$. The dependence of P_1 (c) and $g^{(2)}$ (d) against the optimization constrain $P \geq 2$.

Since the fidelity of single photon filtration (the brightness of the single photon source) is limited as $P_1 < \varphi|\alpha^2|/2$, here we study the performance of the QSF with increasing input power $|\alpha^2|$ numerically. Shown in Fig. S1(a) by solid lines, the probabilities of Fock state outputs P_n $(n = 0, 1, 2, 3, 4)$ against $|\alpha^2|$ is calculated, for $\varphi = 0.1$ and other parameters satisfy the optimal condition Eq. (7). For weak input, the P_1 increases linearly with $|\alpha|^2$ as expected, and $g^{(2)}$ also increases [Fig. S1(b)]. This means that the practical performance of the SPF deviated from the expected perfect single photon source that $g^{(2)} \approx 0$ for $|\alpha^2| \geq 1$. The imperfection for larger input coherent laser intensity should be attributed to the contributions of multiple photons with $n \geq 3$. This can be inferred from the probability of P_2 and P_3 in Fig. S1(a), where the P_2 is approximately linearly depends on P_3. This indicating that the 2-photon output comes from the 3-photon component of input state, which can't be eliminated efficiently by two-unit QSF.

Since the derivation of the optimal conditions is based on the assumption that $|\alpha^2| \ll 1$, the optimal condition may not be valid when increase the input coherent laser power. Therefore, to gain P_1 as large as possible but keep the multiple photon probability as small as possible, we may optimize the parameters of QSF numerically for larger $|\alpha^2|$. For example, we optimize the P_1 under the constrain $P_{n\geq 2} < 0.01(0.001)$, the results are shown by dashed (doted) line in Figs. S1(a) and (b). For $|\alpha^2| \geq 1$, the performance of the QSF in both P_1 and $g^{(2)}$ are improved. For example, with the input mean photon number $|\alpha|^2 = 1$, $P_1 = 0.047$ and $g^{(2)} = 0.48$ for the optimal condition from Eq. (7). With numerical optimization, we obtained the improved performance as $P_1 = 0.18$ and $g^{(2)} = 0.48$ for constrain $P_{n\geq 2} \leq 0.01$ and $P_1 = 0.10$ and $g^{(2)} = 0.22$ for constrain $P_{n\geq 2} \leq 0.001$. It's obvious that, As illustrated in Fig. 2(c) and (d) by comparing the optimized P_1 and $g^{(2)}$ for different constrain $P_{n\geq 2}$, there is a trade-off relation between P_1 and $g^{(2)}$ due to the lack of ability to suppress 2-photon output from multiphoton input state.

II. THE DEPENDENCE ON KERR NONLINEARITY

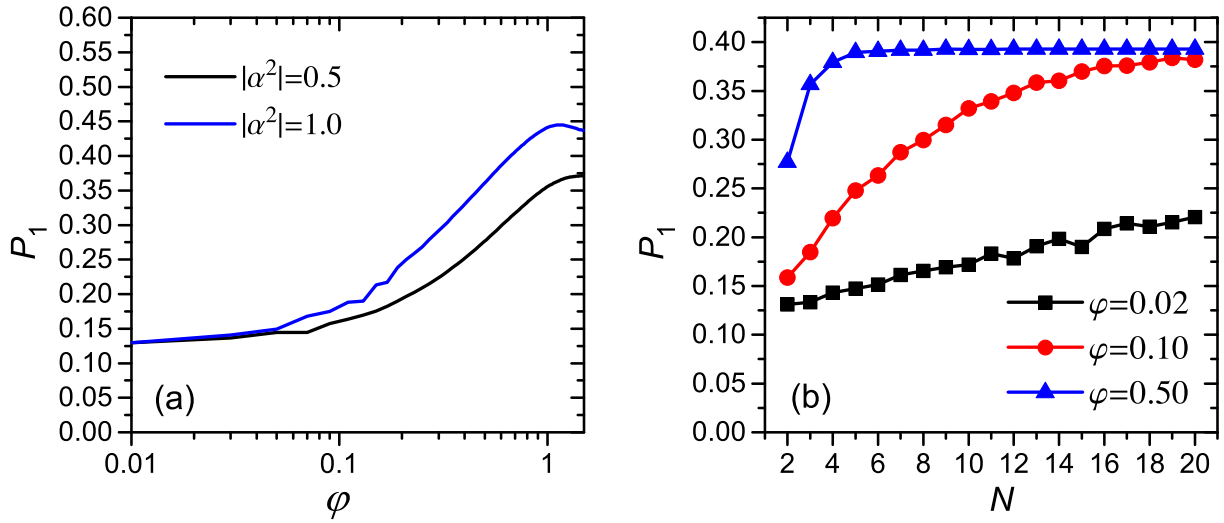

Figure S2: (a) The probability of single photon filtration by QSF against Kerr nonlinearity φ for different input coherent laser intensity $|\alpha^2|$. (b) The probability of single photon extraction by N-unit QSE against unit number N for different φ. All results are optimized under constrains that $P_{n\geq 2} < 0.01$.

In the main body of the paper, most results of QSF are studied for fixed nonlinearity parameter $\varphi = 0.1$. From the results of QSF, the fidelity of single photon filtration is also limited by the Kerr nonlinearity in the NMZI. Therefore, we provide more results to study the dependence of the performance of QSF/QSE on φ.

Shown in Fig. S2(a) are the fidelity of single photon filtration bu QSF against φ for different $|\alpha^2|$. For both $|\alpha^2| = 0.5$ and $|\alpha^2| = 1.0$, the P_1 increase with φ, confirms that the asymptotic formula $P_1 < \varphi|\alpha^2|/2$, indicating that the performance of QSF by the simple NMZI can be improved by larger nonlinearity. By further increase φ, P_1 reaches the saturation value when $\varphi \approx 1$.

In Fig. S2(b), the P_1 by N-unit QSE against N for various φ are studied. It's not surprising that the performance of QSE is also improved by increasing N, and reaches the saturation value $1 - |\langle 0|\alpha\rangle|^2$. Comparing different curves, the higher the nonlinearity is, the less units required to reach the maximum fidelity.

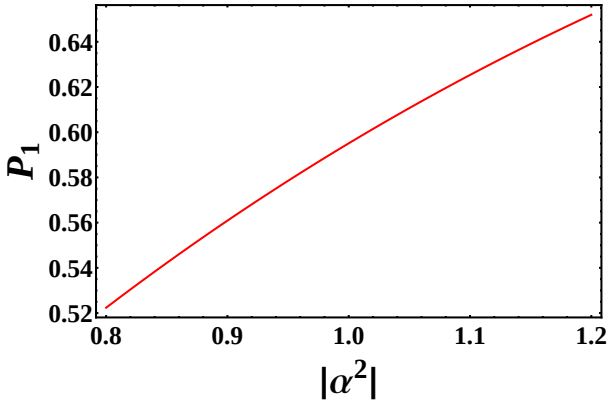

Figure S3: The P_2 for different input coherent laser power.

III. IMPERFECTIONS

To test the performances of QSE against the imperfections of parameters, we studied the performance of the single photon extraction with the optimized parameters for the QSE consist of $N = 20$ units with $|\alpha|^2 = 1.0$ and $\varphi = 0.1$.

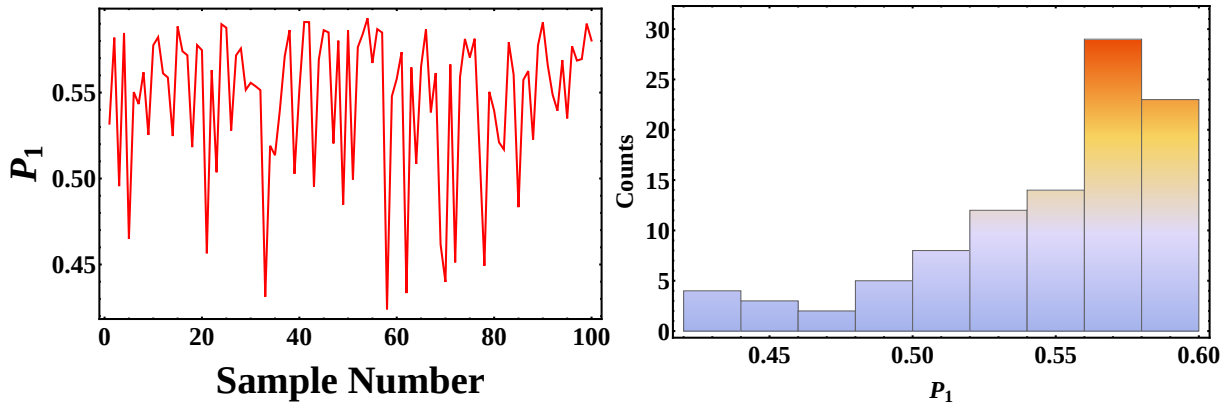

Figure S4: (Left) The P_1 for different samples of varied parameters. (Right) The histogram of the P_1 for the random variation of parameters.

In Fig. S3, the P_1 for varying input coherent laser intensity is shown. In a wide range of input coherent state mean photon number, the P_1 is not deviated much from the optimized value.

In Fig. S4, the P_1 is tested with random perturbations of ϕ and θ from the optimized value. The perturbations are randomly and uniformly distributed in the range from -0.01π to 0.01π. From the results, the performance of the QSE show certain tolerance to the parameter imperfections.

IV. PROOF OF HIGH FIDELITY

As evidences shown in Figs. (2)&(3), the purity and fidelity of the QSF/QSE can approach unitary when $|\alpha|^2$ and N approaches infinity. Here, we provide the analytical analysis to support this argument. In the example, the target state is

$$|\psi_{target}\rangle = (|0\rangle + |1\rangle)/\sqrt{2}. \tag{S.1}$$

In general, the output state can be represent by

$$U\,|0\rangle_A\,|\alpha\rangle_B = |0\rangle_A \sum_{n=0}^{\infty} c_n \zeta_{0,n}\,|n\rangle_B + |1\rangle_A \sum_{n=1}^{\infty} c_n \zeta_{1,n-1}\,|n-1\rangle_B\,, \tag{S.2}$$

where U is unitary transformation, $c_n = \frac{\alpha^n}{\sqrt{n!}} e^{-|\alpha|^2/2}$ for coherent input $|\alpha\rangle$, and the coefficients satisfy $\left|\zeta_{0,n}^2\right| + \left|\zeta_{1,n}^2\right| = 1$. For $N \gg 1$, it's possible to achieve near-perfect extraction of Fock states that generate $\zeta_{0(1),n} = \frac{1}{\sqrt{2}}$ for all n. Then, we obtain the fidelity of the QSE as

$$F = \frac{1}{2}(1 + \sum_{n=0}^{\infty} c_{n+1} c_n^*). \tag{S.3}$$

For $|\alpha^2| \gg 1$, it can be approximated as

$$F \approx 1 - \frac{1}{16|\alpha|^2}, \tag{S.4}$$

where

$$\begin{aligned}
\sum_{n=0}^{\infty} c_{n+1} c_n^* &= \sum_{n=0}^{\infty} \frac{\alpha}{\sqrt{n+1}} \frac{|\alpha|^{2n}}{n!} e^{-|\alpha|^2} \\
&\approx \sum_{n=0}^{\infty} [1 - \frac{n+1-|\alpha|^2}{2|\alpha|^2} + \frac{3}{8}\frac{(n+1-|\alpha|^2)^2}{|\alpha|^4}] \frac{|\alpha|^{2n}}{n!} e^{-|\alpha|^2} \\
&= 1 - \frac{1}{8|\alpha|^2} + \frac{3}{8}\frac{1}{|\alpha|^4}.
\end{aligned} \tag{S.5}$$